Geophysical Research Letters

Supporting Information for

Variation of the Air Mass Exposure to Chlorophyll Over Eastern China Seas: an Insight into Marine Biogenic Aerosols

Shengqian Zhou[1], Ying Chen[1,2*], Fanghui Wang[1], Yang Bao[1], Xiping Ding[3], Zongjun Xu[1]

[1]Shanghai Key Laboratory of Atmospheric Particle Pollution Prevention, Department of Environmental Science & Engineering, Institute of Atmospheric Sciences, Fudan University, Shanghai 200438, China.

[2]Institute of Eco-Chongming (IEC), Shanghai 202162, China.

[3]Pudong New District Environmental Monitoring Station, Shanghai 200135, China.

Corresponding author: Ying Chen (yingchen@fudan.edu.cn)

Contents of this file

Text S1 to S2
Figures S1 to S10

Additional Supporting Information (Files uploaded separately)

Caption for Tables S1

Introduction

This file contains 2 supplementary texts showing detailed information about (1) the field campaigns and chemical analyses, and (2) the data match-up between AEC and marine biogenic MSA for constructing the parameterization scheme. It also contains 10 graphs supporting the methods and main text, as well as the caption for a supplementary table listing historical MSA measurements and relevant information.

Text S1. Cruise campaigns, aerosol sampling, and chemical analyses

We have conducted four seasonal cruise campaigns in the eastern China seas during (1) 27 March to 14 April 2017 (spring), (2) 27 June to 19 July 2018 (summer), (3) 28 December 2019 to 17 January 2020 (winter), and (4) 12 to 29 October 2020 (autumn). Two other cruises in the eastern China seas to WNPO were conducted during (5) 17 March to 23 April 2014 and (6) 30 March to 4 May 2015. The tracks of cruise 1-4 are shown in Figure S2, and the tracks of cruise 5 and 6 can be found in Fu et al. (2018) and Yang et al. (2020) respectively. During the cruises, TSP samples were collected on cellulous filters (Whatman Grade 41) by high-volume samplers with a flow rate of 1.05 m^3 min^{-1}. The duration of each sample was typically 12–24 hours, and the sampling was paused if there was a forward apparent wind or the ship was stopped in order to avoid the exhaust contamination. In each campaign, 2–3 operational blanks were set.

1/32 of each sampling filter was cut and extracted ultrasonically by 20 mL of ultrapure water (> 18.25 MΩ cm^{-1}). The extracting solution was filtered by a polytetrafluoroethylene (PTFE) syringe filter (pore size = 0.45 μm). Then, the concentrations of Na^+, MSA, and SO_4^{2-} were determined by ion chromatography (Thermo, DIONEX ICS-3000). Blank corrections were conducted for all chemical measurements. The ambient mass concentration of nss-SO_4^{2-} was calculated by subtracting sea-salt SO_4^{2-} based on the typical Na^+-to-SO_4^{2-} ratio in seawater: nss-SO_4^{2-} = SO_4^{2-} – 0.251 × Na^+ (Pilson, 2012).
1/16 of each sampling filter was cut was digested with 8 mL of ultrapure HNO_3 and 0.6 mL of ultrapure HF in a microwave digestion system (MARS XPress, CEM). The digested solution was heated and evaporated to about 0.5 mL and then diluted to 15 mL with 2% HNO_3. Then the concentrations of Al and Cd were determined by an inductively coupled plasma mass spectrometry (ICP-MS, NexION 300X, PerkinElmer).

Text S2. Match-up between AEC and marine biogenic MSA

We integrated previously reported MSA measurements and our observations over the eastern China seas (Table S1) and obtained the relationships between MSA concentration and the AEC for each region. As for the 6 cruises we performed (four cruises in the YS and ECS and two cruises in ECS and NWPO), the R_L, AEC, and R_{MBL} for a specific TSP sample were obtained by averaging their values calculated from all trajectories of the sample (trajectory numbers = sampling hours). For autumn and winter cruises, only samples with $R_L < 0.1$ were retained in order to eliminate the impact of terrestrial MSA. For spring and summer cruises, no R_L filtration was applied. Then, the samples with mean $R_{MBL} > 0.9$ were retained and those located in the same region during each cruise were binned. As for other cruise observations collected from previous studies, they were all performed in spring and summer. Because no detailed information about the cruise track history and sampling periods is available, for each cruise, we applied the average AEC value (under the condition of $R_{MBL} > 0.9$) for all 1° × 1° grid cells that ship navigated in a certain region to match the average MSA concentration of all samples. For island-based observations, the AEC (under the condition of $R_{MBL} > 0.9$) in each spring and summer campaign over Huaniao Island and in each month during March to October over Okinawa Island (Zhu et al., 2015) were matched to corresponding average MSA

concentrations. The selection of these campaigns also aims to avoid the significant interference of terrestrial transport.

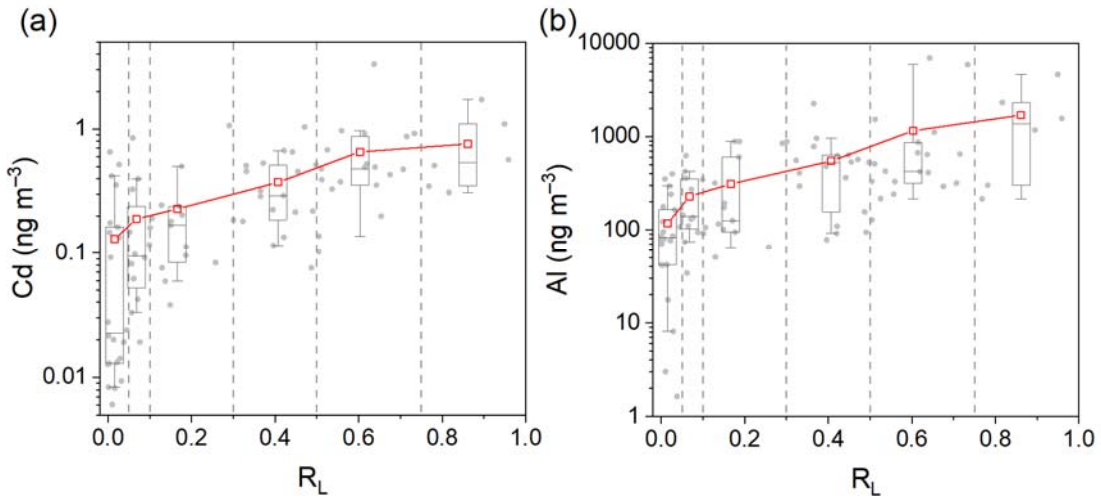

Figure S1. Relationships between (a) Cd and (b) Al concentrations and R_L in four cruises over the eastern China seas during 2017 to 2020. The gray dots represent initial data pairs and the box-whisker plots represent the binned results with R_L boundaries of 0.05, 0.1, 0.3, 0.5, and 0.75, and are drawn for 10-, 25-, 50-, 75-, and 90-percentiles. The red rectangles represent the mean values of each bin.

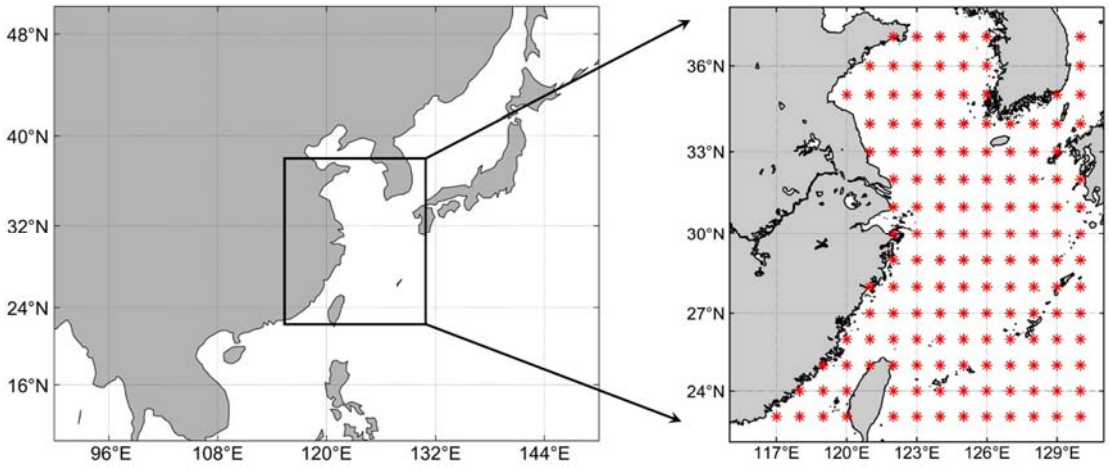

Figure S2. The location of the research region. The red star represents the center of each grid.

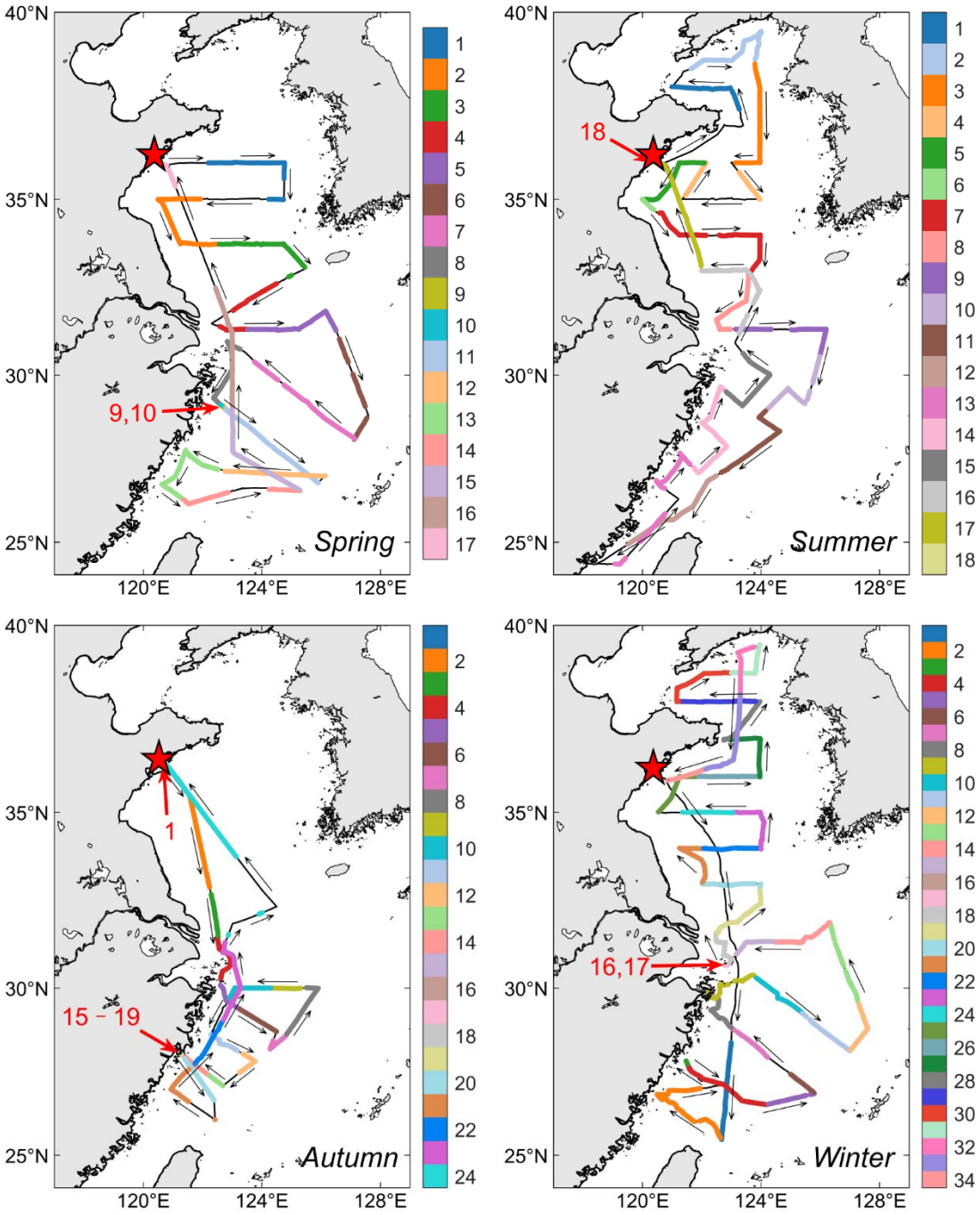

Figure S3. The tracks of cruise 1–4 in the eastern China seas. The cruise segments with different colors correspond to different samples, and the sample IDs are listed as legends. The red star represents the home port of research vessels.

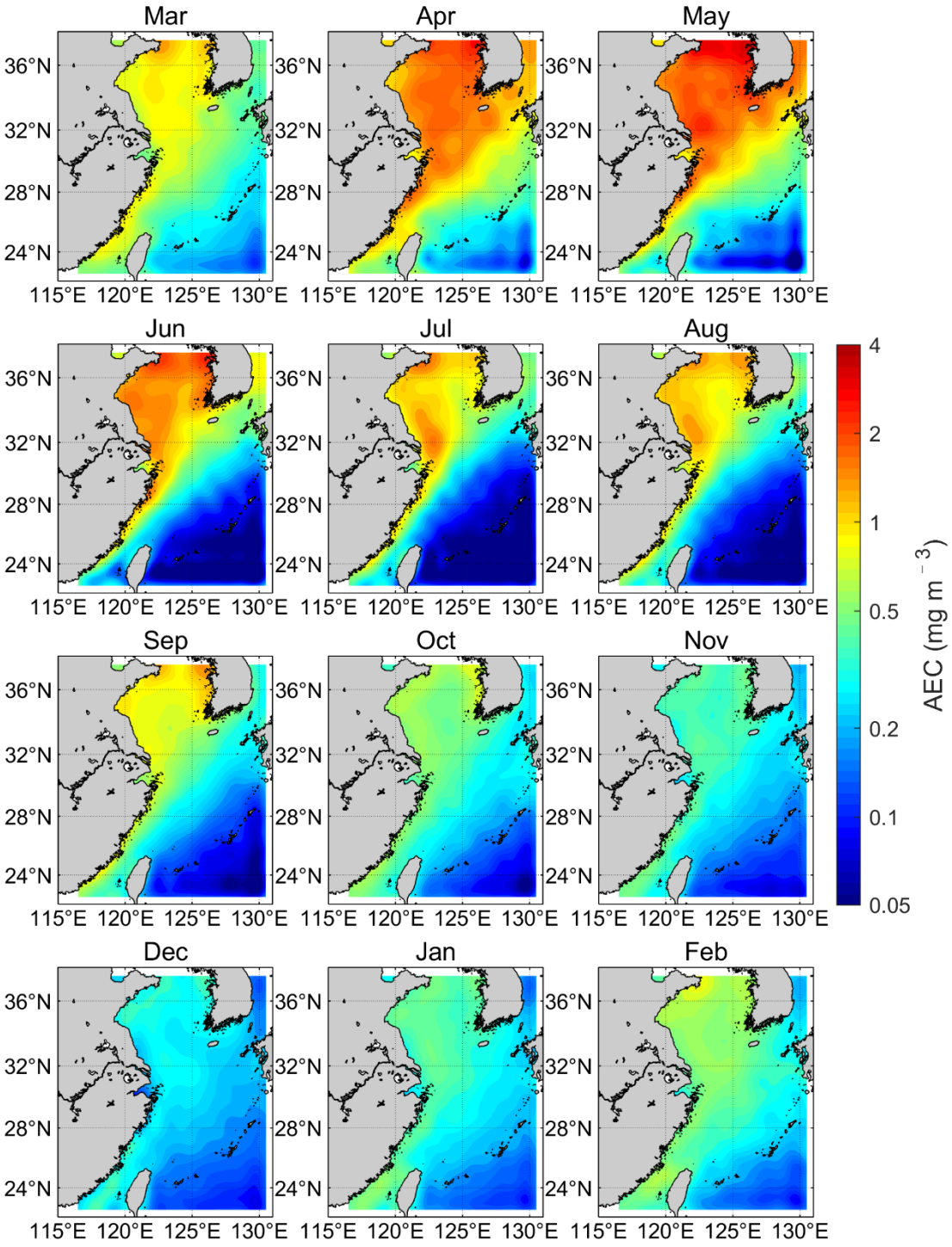

Figure S4. Monthly climatology for AEC under the condition of R_{MBL} > 0.9 during 2009 to 2020.

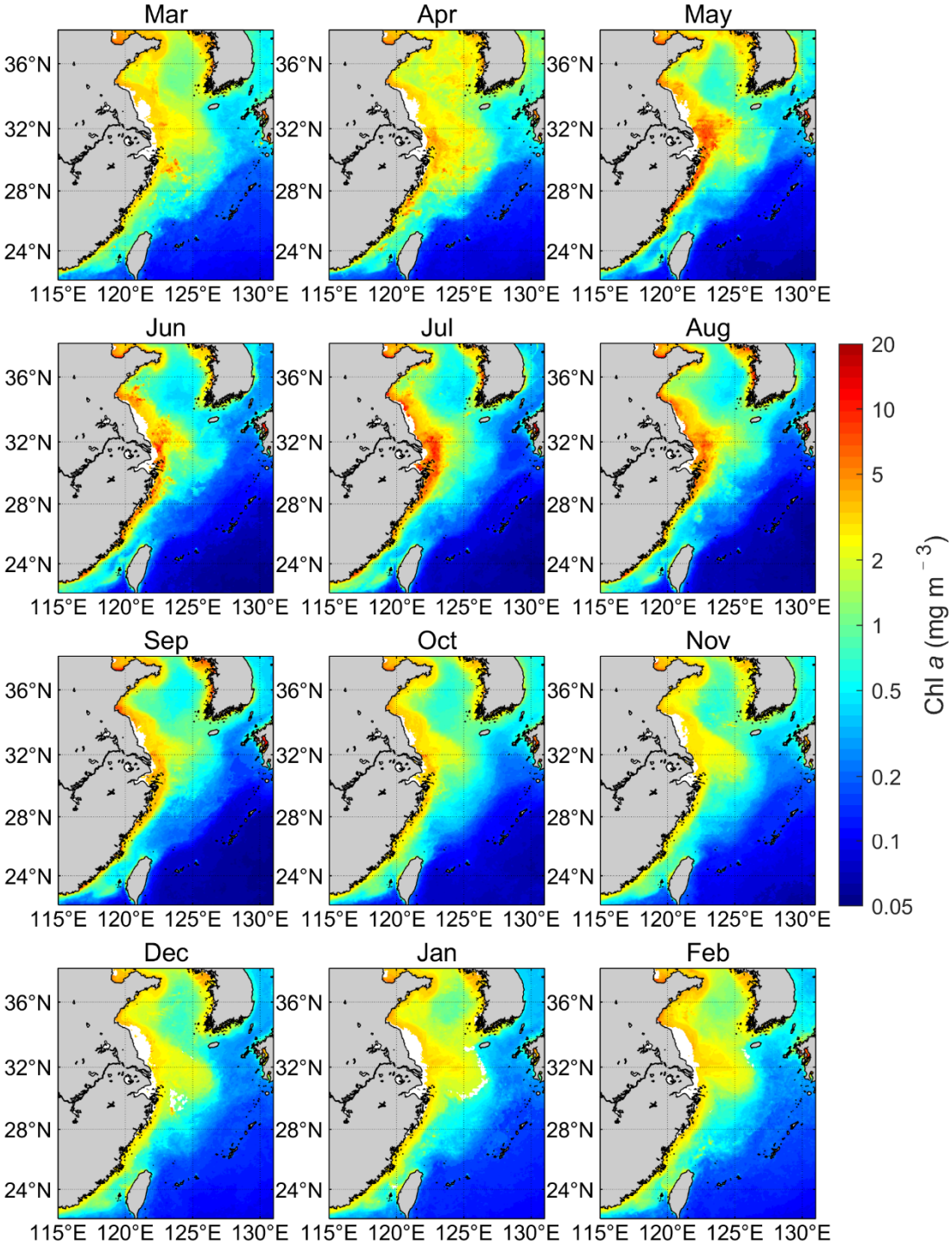

Figure S5. Monthly climatology for the concentration of sea surface Chl *a* during 2009 to 2020.

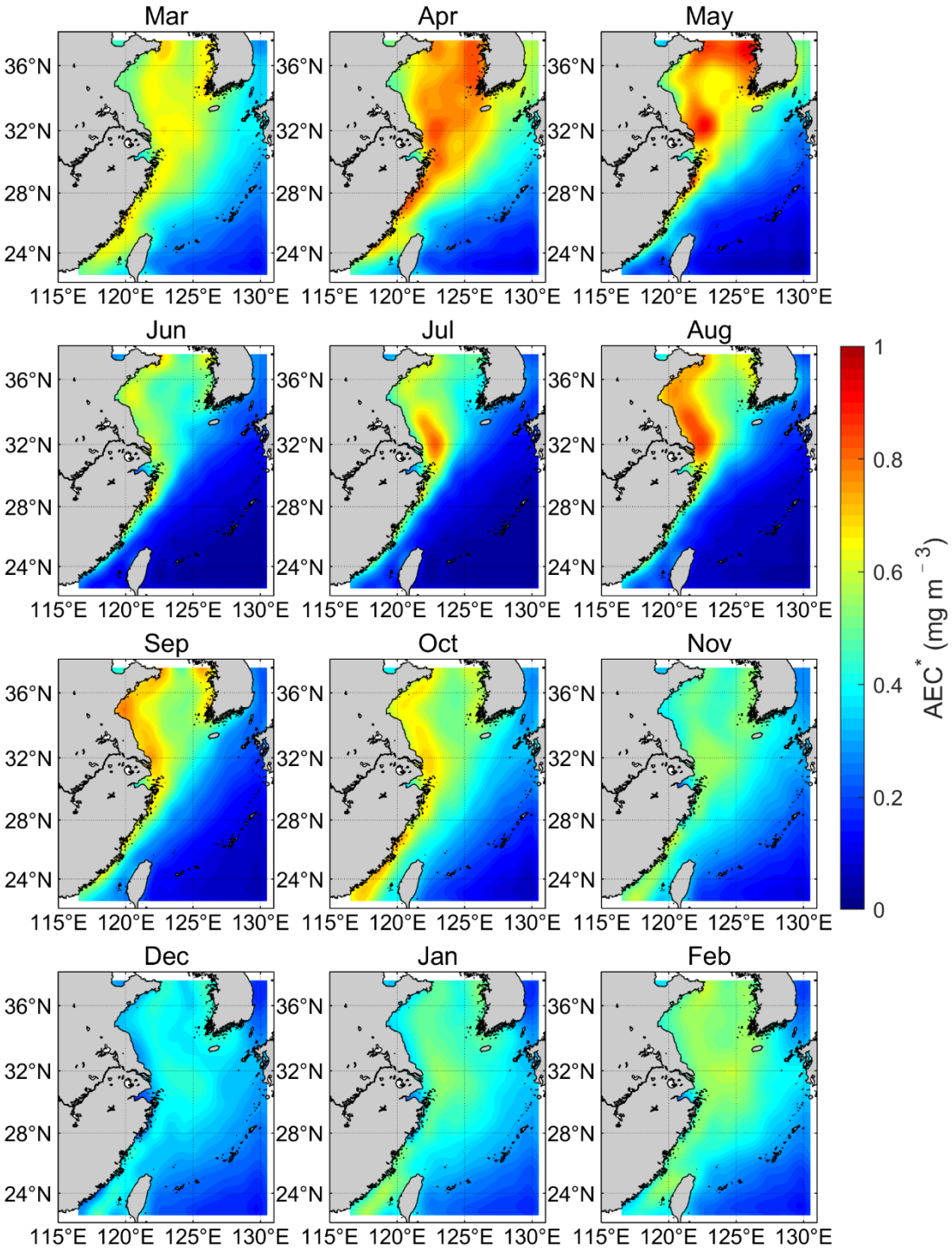

Figure S6. Monthly climatology for AEC index without considering BLH (AEC*) under the condition of R_{MBL} > 0.9 during 2009 to 2020.

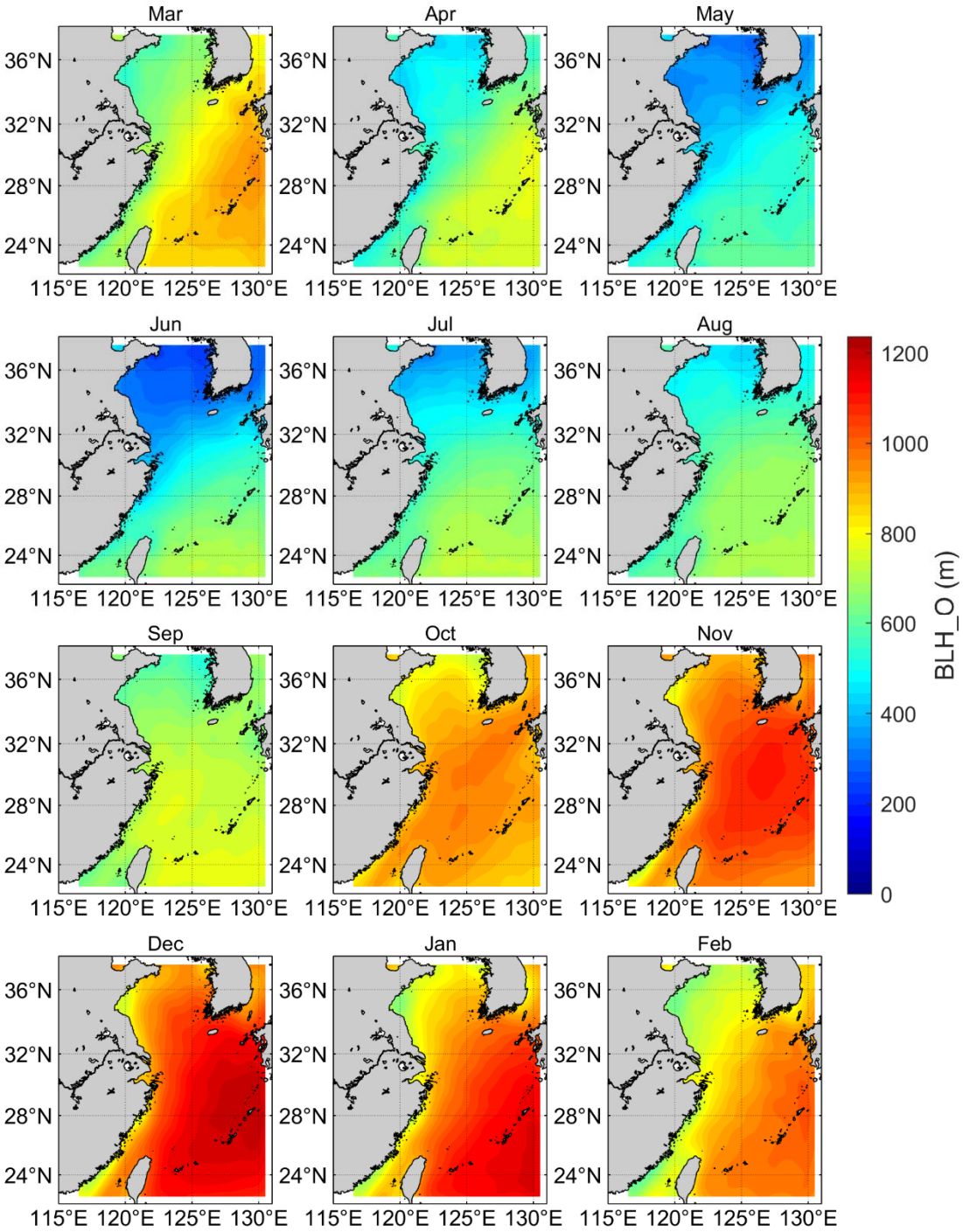

Figure S7. Monthly climatology for BLH along marine trajectory (BLH_O) under the condition of $R_{MBL} > 0.9$ during 2009 to 2020.

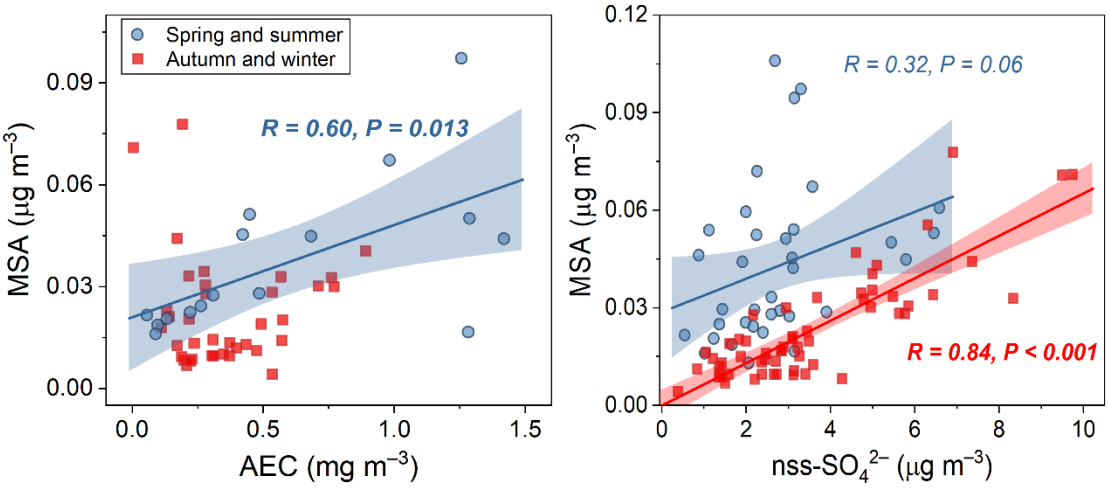

Figure S8. The correlations between MSA concentration and AEC when marine air masses are transported mostly within boundary layer (R_{MBL} > 0.9) and between MSA and nss-SO_4^{2-} concentrations in four cruises over the eastern China seas. The blue markers represent data in the spring and summer, while the red markers represent autumn and winter. The thick lines and shaded bands show the linear regressions and their 95% confidence intervals.

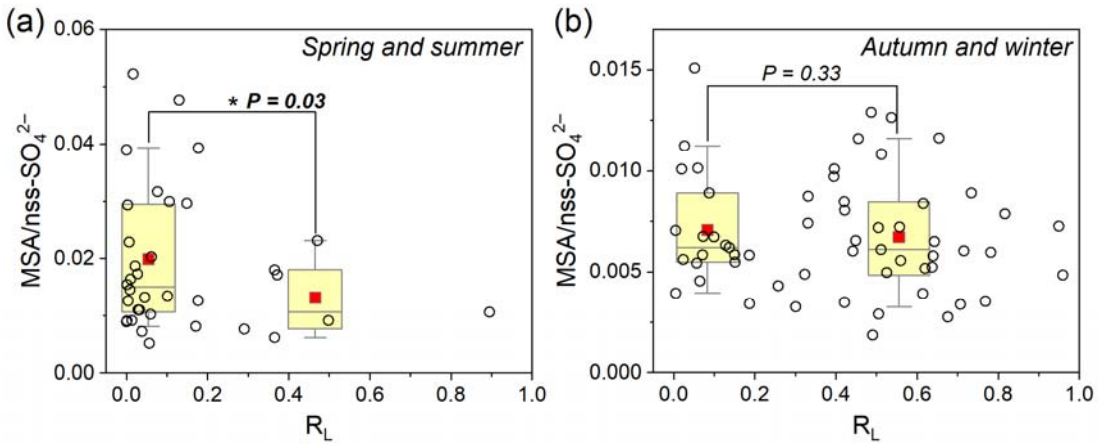

Figure S9. Comparisons between MSA/nss-SO_4^{2-} in different R_L ranges for (a) spring and summer cruises and (b) autumn and winter cruises. The box-whisker plots represent the data distributions with $R_L \leqslant 0.2$ and $R_L > 0.2$, and are drawn for 10-, 25-, 50-, 75-, and 90-percentiles. The red rectangles represent the mean values of each R_L range. The *P* value of the unpaired two-tailed Student's *t*-test is given.

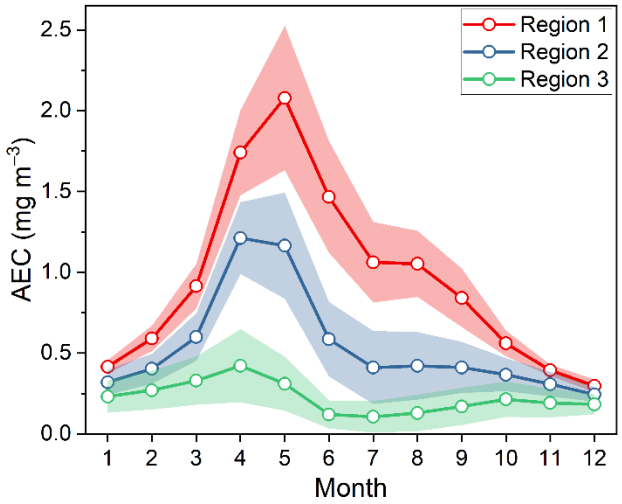

Figure S10. The average AEC for each region in different months. The shaded band denotes the mean ± SD.

Table S1. The information about historical MSA observations used in this study.